Research Square

Preprints are preliminary reports that have not undergone peer review.
They should not be considered conclusive, used to inform clinical practice,
or referenced by the media as validated information.

# Morphometry, Innervation Variability, and Dynamic Nerve Positioning of the Subscapularis Muscle During Shoulder Rotation: A Cadaveric Study

**Amit Kumar Shreevastava**
All India Institute of Medical Sciences Raebareli
**Rajat Subhra Das**
anat_rajat@aiimsrbl.edu.in
All India Institute of Medical Sciences Raebareli
**Thummala Naveen Sagar**
All India Institute of Medical Sciences Raebareli

**Research Article**

**Keywords:** Subscapularis muscle, Subscapular nerve, Innervation variability, Subscapularis superior–inferior belly axis angle, Footprint, Myotendinous junction, Shoulder rotation

**Posted Date:** September 10th, 2026

**DOI:** https://doi.org/10.21203/rs.3.rs-10826930/v1

**License:** This work is licensed under a Creative Commons Attribution 4.0 International License.
Read Full License

**Additional Declarations:** No competing interests reported.

**Title:** Morphometry, Innervation Variability, and Dynamic Nerve Positioning of the Subscapularis Muscle During Shoulder Rotation: A Cadaveric Study.

**Authors:**

Principal Investigator**:** Dr. Amit Kumar Shreevastava
Associate Professor
Department of Anatomy
All India Institute of Medical Sciences, Raebareli
ORCID ID: 0000-0002-4488-7921
Email: anat_amit@aiimsrbl.edu.in

Co-Investigators: Dr. Rajat Subhra Das
Professor & Head
Department of Anatomy
All India Institute of Medical Sciences, Raebareli
ORCID ID: 0000-0002-7143-8662
Email – anat_rajat@aiimsrbl.edu.in

Dr. Thummala Naveen Sagar
Associate Professor
Department of Anatomy
All India Institute of Medical Sciences, Raebareli
ORCID ID: 0000-0003-1465-0197
Email: anat_naveen@aiimsrbl.edu.in

Corresponding author - Dr. Rajat Subhra Das, Professor & Head, Department of Anatomy
All India Institute of Medical Sciences, Raebareli.
Email – anat_rajat@aiimsrbl.edu.in

**Acknowledgement** – We are grateful to the authority of the Institute for providing the necessary resources and facilities and the staff of the Department of Anatomy for their support.

**Funding** - There was no kind of funding towards conducting this study.

**Conflict of interest** – Authors declare that there is no conflict of interest.

**Authors contributions**

Dr. Amit Kumar Shreevastava has contributed in conceptualization, study design, and data collection and analysis, writing the manuscript.

Dr Rajat Subhra Das has supervised the research project, study design and provided oversight in methodology, and contributed to the final manuscript draft.

Dr. Thummala Naveen Sagar has assisted in the data collection process, contributed to statistical analysis, and writing the manuscript.

## Abstract

The subscapularis muscle (SM) shows considerable variation in its musculotendinous structure and nerve supply, which may influence shoulder biomechanics and increase the risk of nerve injury during glenohumeral joint surgeries. This cadaveric study evaluated the morphometry, innervation patterns, subscapularis superior–inferior belly axis angle (SSIBAA), and rotation-dependent positional changes of the subscapular nerves in Type III and Type IV SM. Forty-six upper limbs from 23 embalmed adult cadavers were examined. The SM morphometric measurements, SSIBAA, and the origin and branching pattern of the subscapular nerves were documented. Distances from the entry points of the upper and lower subscapular nerves to the myotendinous junction (MTJ) were measured with the shoulder abducted to 30° in neutral, external, and internal rotations. Type IV SM was observed more often than Type III SM (56.5% vs. 43.5%). Type IV had significantly greater footprint length, MTJ width, muscle height, scapular height, and SSIBAA than Type III. The upper subscapular nerve originated from the posterior cord, whereas the lower subscapular nerve showed variable origins. Accessory upper subscapular nerves were significantly more frequent in Type IV. In both SM types, the shortest distance from the nerve entry point to the MTJ was greatest during external rotation, intermediate during neutral rotation, and shortest during internal rotation. These findings enhance the anatomical understanding of SM morphology and innervation patterns and improve surgeons' understanding of an anatomically safe zone, thereby minimizing intraoperative injury to the subscapular nerves during an anterior glenohumeral joint approach.



**Keywords:** Subscapularis muscle, Subscapular nerve, Innervation variability, Subscapularis superior–inferior belly axis angle, Footprint, Myotendinous junction, Shoulder rotation.

**1 Introduction**: The subscapularis muscle (SM) is an integral component of the rotator cuff muscles (Morag et al. 2011; Alilet et al. 2016; Zielinska et al. 2021). The SM comprises both muscular and tendinous components (Zielinska et al. 2021). The SM originates from the concave subscapular fossa and inserts primarily as a flattened tendon onto the lesser tubercle of the humerus. The inferior-most muscle belly contributes a muscular insertion onto the inferior portion of the lesser tubercle and the adjacent medial lip of the proximal intertubercular (bicipital) sulcus, superior to the teres major muscle's insertion (Morag et al. 2011; Alilet et al. 2016; Siwetz et al. 2021; Zielińska et al. 2021). The SM origin and insertion were highly variable (Zielinska et al. 2021; Mann et al. 2023). The upper subscapular nerve (USN) innervates the upper two-thirds of the SM, and the lower subscapular nerve (LSN) innervates the lower one-third. Usually, the posterior cord of the brachial plexus gives rise to both the nerves (Tubbs et al. 2007; Kasper et al. 2008; Alilet et al. 2016; Sager et al. 2019). Some studies have documented variability in the innervation pattern of the SM (Tubbs et al. 2007; Kasper et al. 2008; Leschinger et al. 2016; Siwetz et al. 2021). In previous cadaveric research, the SM was classified based on muscle bellies. It may range from a single belly to nine bellies (Types I to IX), with the three-bellied (Type III) variant the most common (31.9%), followed by the four-bellied (Type IV) variant (30.3%) (Zielińska et al. 2021). In another prior study, SM classification depended on the number of tendons present. The single-tendon (Type I) pattern was observed in 43.7% of specimens, the four-tendon (Type IV) pattern in 39.1%, the two-tendon (Type II) pattern in 9.4%, and the three-tendon (Type III) pattern in 7.8% of cases (Zielinska et al., 2021). Until now, the SM has been categorized separately, either because of multiple tendons or muscular bellies (Zielińska et al., 2021). By contrast, our classification relies on the number of tendon–muscle belly units, with each separate muscle belly forming a corresponding tendinous slip.

The multipennate architecture of the SM may have evolved as an adaptation to the increasing functional demands on the shoulder over time. This arrangement improves force generation, range of motion, and movement precision, but may compromise tendon strength. The evolution of brachiation and later bipedal posture may have shaped this muscle's design to maintain dynamic stabilization of the glenohumeral joint (GHJ) and support complex, precise, and varied movements (Zielińska et al. 2021).

The SM is the biggest and strongest rotator cuff (RC) muscle (Alilet et al. 2016; Mann et al. 2023). It mainly functions as an internal (medial) rotator, setting it apart from the other rotator cuff muscles (Zielinska et al. 2021). Across different arm positions, the SM may act as an adductor, abductor, extensor, and flexor (Morag et al. 2011; Mann et al. 2023). The upper part of the muscle fibers primarily performs abduction, the middle portion assists in medial rotation, and the lower part is involved in adduction (Alilet et al. 2016; Mann et al. 2023). Electromyographic studies have found the superior part of the SM to be more active than the lower portion during shoulder elevation, supporting its role in abduction (O'Connell et al. 2006; Zielińska et al. 2021). The SM works in coordination with the other RC muscles to provide GHJ stability and perform diverse motions. The SM stabilizes the shoulder joint through both

active and passive mechanisms (Morag et al. 2011; Alilet et al. 2016). The SM actively stabilizes the GHJ during external rotation, abduction, extension, and flexion (Halder et al. 2000; Morag et al. 2011; Alilet et al. 2016; Mann et al. 2023). The upper part of the SM counteracts external rotation by acting against the infraspinatus muscle in the axial plane, while the inferior muscle fibers oppose the deltoid-mediated elevation of the humeral head in the coronal plane (Halder et al. 2000; Alilet et al. 2016). Since the lower muscular portion of the SM and its tendon passively maintain anterior shoulder joint stability, muscular laxity or a tendon tear can lead to anterior shoulder joint dislocation (Alilet et al. 2016). Successful treatment of anterior GHJ instability requires accurate repair of the lower subscapularis muscle and tendon (Halder et al. 2000; Morag et al. 2011; Alilet et al. 2016). Finally, the multipennate nature of the SM and its tendons inserting on the footprint enable it to perform multiple functions across variable arm positions while maintaining GHJ stability.

The anterior or deltopectoral approach facilitates a broad surgical view of the GHJ and surrounding structures and is widely used for total shoulder arthroplasty, reverse total shoulder arthroplasty, GHJ instability repair, and RC repair (Leschinger et al. 2017). In the anterior approach to shoulder arthroplasty, the subscapularis tendon and the anterior capsule are released to facilitate adequate exposure of the glenohumeral joint (Sager et al. 2019). The subscapularis tendon may be released using several techniques, including subscapularis peeling, lesser tubercle osteotomy, subscapularis tenotomy, and splitting along the orientation of the subscapularis muscle fiber (Sager et al. 2019; Virk et al. 2019; Siwetz et al. 2022). Even after successful surgery and optimal tendon healing, some patients still show limited recovery of subscapularis function (Leschinger et al. 2017; Sager et al. 2019; Siwetz et al. 2022). Proper arm positioning and its relationship to the subscapularis myotendinous junction (MTJ) are critical during this procedure because the nerve-muscle relationship is highly dynamic and the innervation point is very close to the MTJ. Unsatisfactory subscapularis function may be due to damage to the USN, LSN, and their accessory branches during surgical procedures, which innervate the pennate muscle near the MTJ (Leschinger et al. 2017; Sager et al. 2019; Siwetz et al. 2022). Previous cadaveric studies reported that the innervation points of the USN and LSN within the SM vary across different arm positions. Some published articles documented that during external rotation, the nerve-muscle entry distance, measured from a reference point, increased (Leschinger et al. 2017; Sager et al. 2019), while others reported that it decreased (Kasper et al. 2008). Siwetz et al. (2022) also did a study at 60° and 90° abduction of the arm and found that in both conditions, the distance measured between the nerve-muscle entry point of USN and LSN in SM from MTJ was increased in external rotation of the shoulder and decreased in internal rotation.

Our study aims to provide morphometric details of the SM, describe the variable innervation pattern and subscapularis superior–inferior belly axis angle (SSIBAA), analyze the dynamic nerve-muscle association across different GHJ rotations (neutral rotation, external rotation, and internal rotation) in relation to the MTJ, defining an anatomical safe zone, and discuss its clinical importance.

**2. Materials and methods:** The study was conducted following approval from the Institute's Ethics Committee. It was conducted in the Institute's Department of Anatomy, examining dissected cadaveric specimens from 46 upper limbs of 23 donor cadavers (18 male, 5 female). The cadavers' ages ranged from 65 to 74 years.

**Inclusion criteria**: Formalin-embalmed, well-preserved cadavers were selected for this study. The included cadavers had well-preserved shoulder joints with their rotator cuff component and nearby nerves and vessels. This facilitated thorough dissection and accurate measurement of the anatomical structures. Because the GHJ remained intact, the arm could be positioned consistently at 30° abduction in neutral, external, and internal shoulder rotation during nerve dynamic position analysis.

**Exclusion criteria:** We excluded the cadaveric shoulders having evidence of prior surgery, traumatic injury, fractures, congenital anomalies, gross deformities, or pathological changes involving the scapula, glenohumeral joint, or proximal humerus. During dissection, if we encountered a damaged subscapularis muscle or subscapular nerves, or found it difficult to fully expose the subscapularis muscle and its nerve supply, we also excluded those specimens because this could compromise the reliability of the morphometric and neuroanatomical measurements.

**2.1 Dissection procedure:**

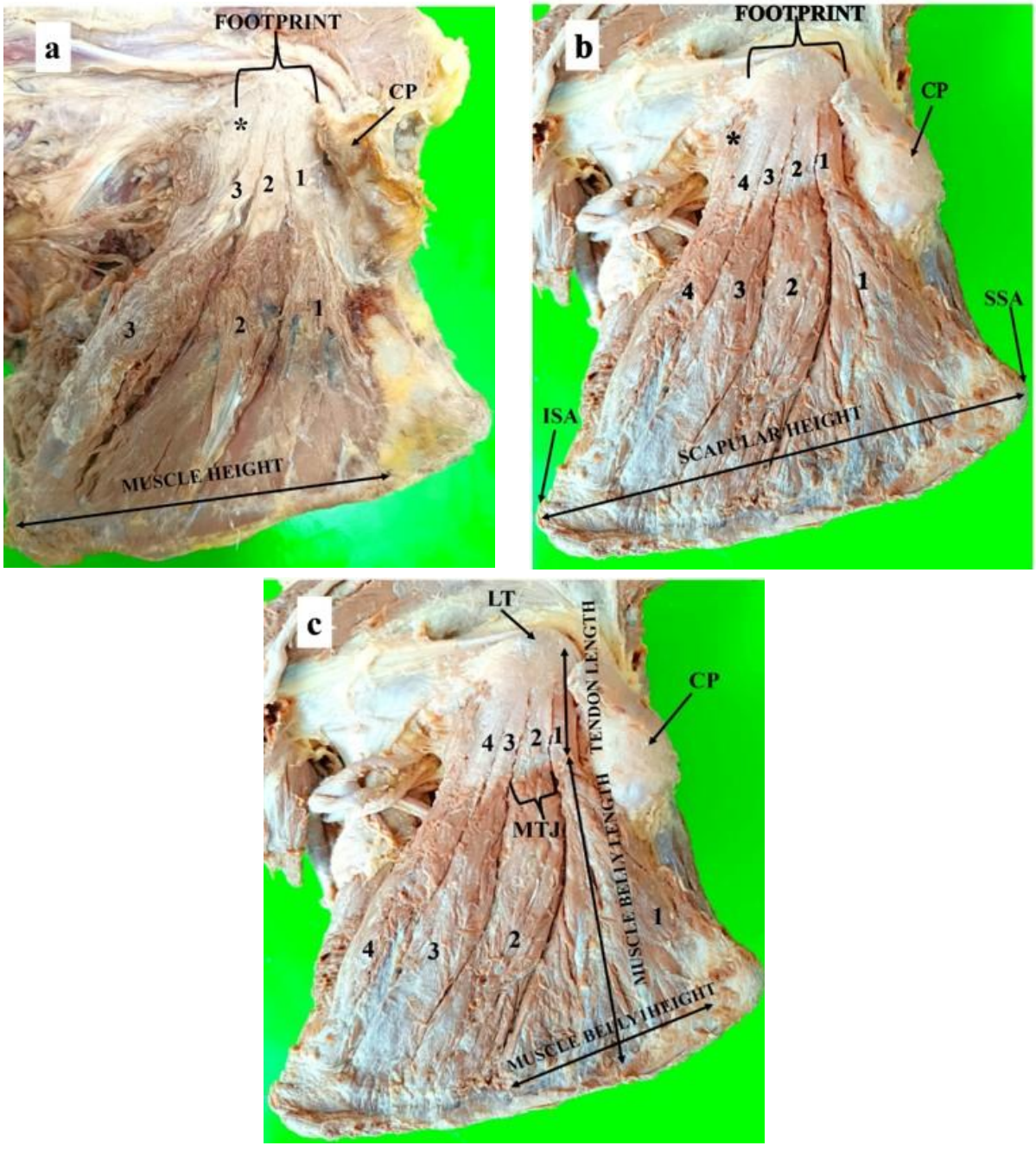
A modified extended deltopectoral dissection was carried out to expose the shoulder region and associated neurovascular structures. The pectoralis major muscle was dissected out from its humeral insertion and clavicular origin and reflected medially. The deltopectoral interval was developed, and the clavipectoral fascia was incised. Further, the deltoid muscle was removed from its clavicular and acromial origins and reflected distally to expose the anterior aspect of the glenohumeral joint. Later, we freed the pectoralis minor muscle from its insertion on the coracoid process to expose the axillary artery, the cords of the brachial plexus, and their branches. The surrounding fat and fascia were carefully removed to expose and preserve the posterior cord, USN, LSN, thoracodorsal nerve, and axillary nerve. The SM was completely exposed from its scapular origin to its insertion on the lesser tubercle and the adjacent medial lip of the intertubercular (bicipital) groove by carefully removing the surrounding connective tissue while preserving its tendon–muscle belly architecture and neurovascular supply. The connective tissue over the MTJ was carefully removed to enable accurate visualization for morphometric measurements. The anterior capsule of the GHJ was exposed to permit complete visualization of the subscapularis tendon insertion (footprint). During dissection, the GHJ and surrounding soft tissues were kept intact, allowing the arm to remain standardized at 30° abduction in neutral, external, and internal rotation for neuroanatomical measurements. The origin, course, branching pattern, anatomical variations, and muscle penetration points of the USN and LSN, including their accessory branches, were carefully documented before morphometric and neuroanatomical measurements were performed.

**2.2 Classification**:

After anatomical dissection, the subscapularis muscle was carefully examined to study its tendon and muscle belly structure. The number of separate tendons attaching to the lesser tubercle was counted, and each tendon was followed back to its muscle belly. Each tendon and

its muscle belly were treated as one tendon–muscle belly unit. We numbered the muscle bellies from top to bottom based on where their tendons attached. Specimens with three tendon–muscle belly units were labeled as Type III, and those with four were labeled as Type IV (Figure 1).

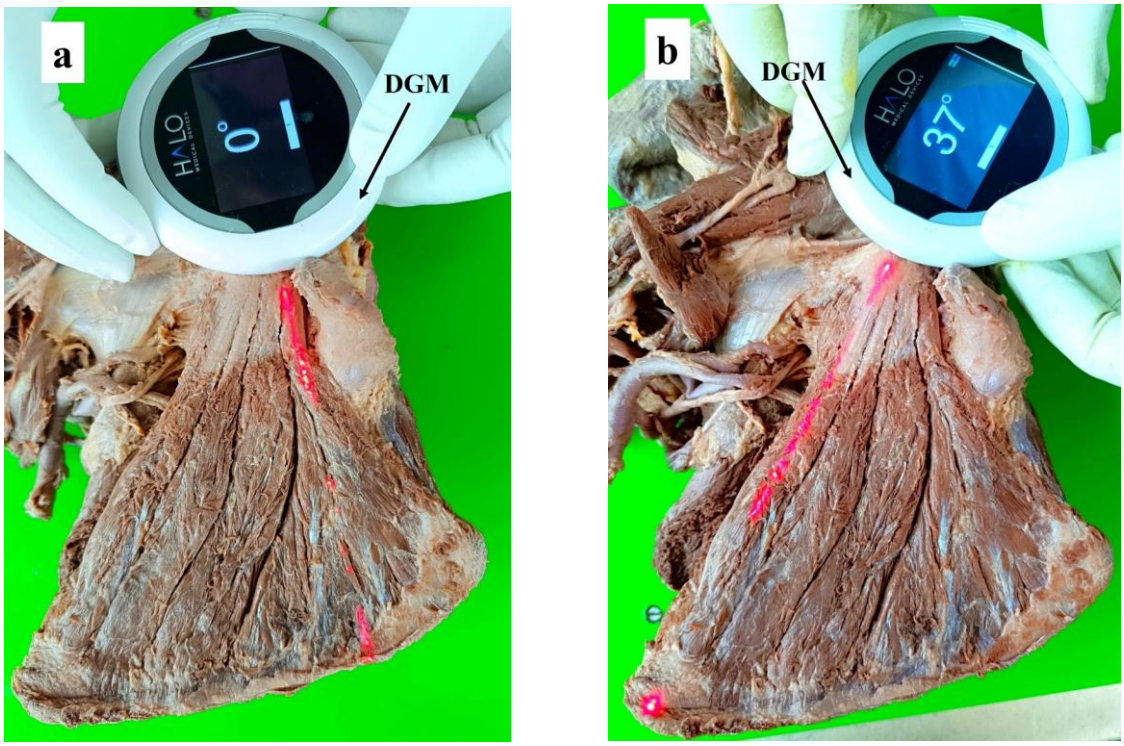
**FIGURE 1**: **(a)** Type III and **(b)** Type IV subscapularis muscles in cadaveric specimens. **(c)** Representative morphometric measurements performed on a Type IV subscapularis muscle. The same measurement protocol was used for both Type III and Type IV muscles. Tendons and their corresponding muscle bellies are numbered sequentially from superior to inferior (1–4). The asterisk (*) indicates the muscular attachment of the inferior-most subscapularis muscle belly. Abbreviations: MTJ, myotendinous junction; LT, lesser tubercle; CP, coracoid process; SSA, superior scapular angle; ISA, inferior scapular angle.



**2.3 Morphometric measurements of the subscapularis muscle:** We used a digital Vernier caliper (accuracy 0.01 mm) to measure morphometric details. After complete exposure of the muscle, the number of distinct tendons inserting onto the lesser tubercle was recorded, and each individual tendon was traced proximally to its corresponding muscle belly. Tendons and their corresponding muscle bellies were numbered sequentially from superior to inferior according to their anatomical arrangement (Figure 1). Length of the tendon was measured from the MTJ to the closest insertion point on the lesser tubercle. Tendon width and thickness were measured at the junction with the corresponding MTJ. The width of the MTJ was measured at the transition between the muscle belly and its corresponding tendon. The humeral footprint was defined as the entire insertional area of the subscapularis extending from the lesser tubercle to the adjacent medial lip of the proximal intertubercular (bicipital) sulcus. Humeral footprint length was measured as the maximum cranio-caudal length of the insertional area (Figure 1). Muscle height was measured as the maximum straight-line distance between the highest and lowest attachment of the SM along the medial border of the scapula (Figure 1a). The scapular height was measured as the linear distance between the superior and inferior angles of the scapula (Figure1b). Individual muscle belly height was measured as the maximum straight-line distance between the highest and lowest attachment of the corresponding muscle belly along the medial border of the scapula. The midpoint of the individual muscle belly height was identified and used as the reference point for measuring muscle belly length. The length of each muscle belly was measured as the straight-line distance from the midpoint of the individual muscle belly height to the midpoint of the corresponding myotendinous junction (Figure 1c). Each specimen was placed in a standardized anatomical position before measurements were taken using specified anatomical landmarks. Two observers recorded each measurement separately. We averaged the readings for statistical analysis.

**2.4 Subscapularis superior–inferior belly axis angle (SSIBAA) measurement:** The angle between the longitudinal axes of the subscapularis superior and inferior muscle bellies (SSIBAA) was measured using a laser-guided digital goniometer. We placed the goniometer at the midpoint of the subscapularis tendon footprint on the humerus's lesser tubercle. The goniometer's laser ray was aligned with the central longitudinal axes of the superior-most and inferior-most muscle bellies. The ray extended through the tendon to the corresponding MTJ and the corresponding muscle belly. The angle between the two longitudinal axes was expressed in degrees. Two observers independently recorded each measurement, and the average of the two readings was used for statistical analysis (Figure 2).

**FIGURE 2**: **(a, b)** Representative digital measurement of the angle between the longitudinal axes of the superior and inferior muscle bellies in a Type IV cadaveric specimen of the subscapularis muscle. The same measurement protocol was used for both Type III and Type IV muscles. The red laser line was aligned with the longitudinal axis of each muscle belly to determine the angle between the two axes. The measured angle was displayed digitally in degrees. Abbreviations: DGM, laser-guided digital goniometer.

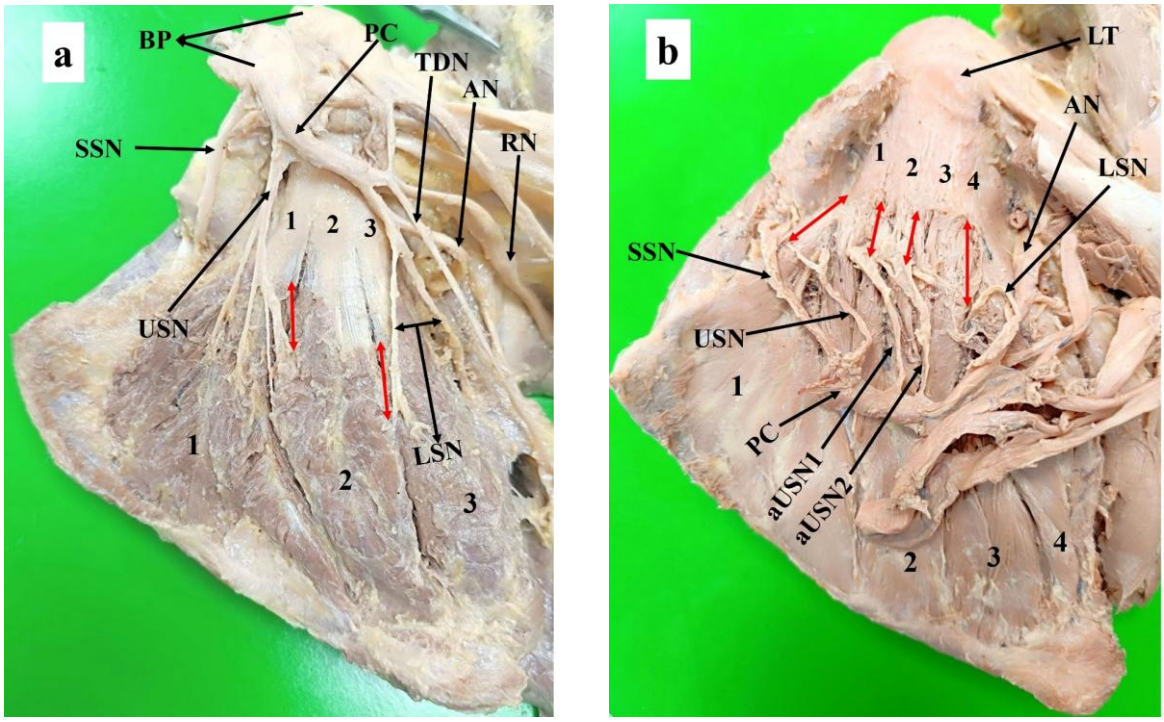



**2.5 Neuroanatomical measurements during shoulder rotation:**

After complete exposure of the SM and its nerve supply, the scapula, GHJ, and proximal humerus were kept intact during all neuroanatomical measurements. The shoulder was kept at 30° of abduction during all measurements to standardize specimen positioning. A digital goniometer was utilized to measure the angle. This position was selected because it provides adequate exposure of the anterior GHJ and SM and less traction on the brachial plexus during the deltopectoral approach, and is similar to prior studies evaluating the subscapular nerve (Walley et al. 2019). The GHJ was then moved sequentially into neutral rotation, external rotation, and internal rotation. After that, the GHJ was moved sequentially into neutral rotation, external rotation, and internal rotation. In each rotational position, the USN and LSN entry points into the subscapularis muscle were identified. For each nerve, the nearest point on the MTJ to the nerve entry point was identified, and the shortest straight-line distance between

these two was measured using a digital Vernier caliper (accuracy, 0.01 mm). In specimens with accessory branches of the USN or LSN, the nerve branch with the entry point closest to the MTJ was selected, and the shortest straight-line distance between its entry point and the nearest point on the MTJ was measured. Accordingly, the recorded measurement represented the neural structure closest to the MTJ within the USN or LSN group. Measurements were obtained without disturbing the anatomical course of the nerves or the integrity of the surrounding soft tissues. The same measurement protocol was consistently used for both Type III and Type IV SM. Two observers acquired each measurement independently, and the average value was used for statistical analysis. After completion of all measurements, representative specimens were carefully removed with the scapula, the intact shoulder joint with the upper limb, the SM, and both the USN and LSN (including any accessory branches, if present). These were used to photograph the measurement technique (Figure 3). Siwetz et al. (2022) did not notice a significant difference in the median distance from the MTJ to the nerve entry point between embalmed and fresh specimens.

**FIGURE 3**: (a) Type III and (b) Type IV subscapularis muscles in representative cadaveric specimens demonstrating the technique used to measure the shortest straight-line distance from the MTJ to the nerve penetration points of the USN, LSN, and accessory upper subscapular nerve branches. Red double-headed arrows indicate the measured distances. Representative specimens were photographed after en bloc removal of the scapula, glenohumeral joint, and proximal humerus to facilitate visualization of the measurement technique. Abbreviations: MTJ, myotendinous junction; BP, brachial plexus; PC, posterior cord; SSN, suprascapular nerve; USN, upper subscapular nerve; aUSN1, first accessory upper subscapular nerve; aUSN2, second accessory upper subscapular nerve; LSN, lower subscapular nerve; AN, axillary nerve; TDN, thoracodorsal nerve**.**




**2.6 Statistical analysis**: We carried out the statistical analysis in Microsoft Excel 2019 using the Analysis ToolPak add-in. Continuous data are represented as mean ± standard deviation (SD). The Shapiro–Wilk test confirmed that all continuous variables were normally distributed. To compare the right and left sides, we used a paired t-test. Since no significant differences were found, bilateral data were combined for comparisons between Type III and Type IV SM, using Welch's unpaired t-test. One-way repeated-measures ANOVA was followed by Bonferroni post hoc comparisons to assess the tendon and muscle belly measurements in both muscle types. The association between accessory upper subscapular nerves (aUSN) and muscle type was analyzed with the Pearson chi-square test. Pearson's correlation was used to analyze relationships among selected morphometric parameters, and simple linear regression was conducted to evaluate these findings. A p-value of $\leq 0.05$ was regarded as significant, with adjusted thresholds for Bonferroni tests.

## 3 Results:

### 3.1 Classification of the subscapularis muscle:

A total of 46 subscapularis muscles from 23 cadavers (18 male, 5 female) were examined. Based on tendon–muscle belly architecture, 26 specimens (56.5%) were classified as Type IV and 20 (43.5%) as Type III, indicating that Type IV was the predominant morphological pattern in this study.

### 3.2 General morphometric parameters:

No significant differences were observed between the two sides in footprint length, MTJ width, muscle height, scapular height, or SSIBAA in either Type III or Type IV SM. Because no

significant bilateral differences were observed, bilateral data have been pooled for subsequent comparisons across the SM types (Table 1).

### 3.3 Comparison between Type III and Type IV subscapularis muscles:

Type IV SM showed significantly greater footprint length, MTJ width, muscle height, scapular height, and SSIBAA than Type III SM. No significant differences were observed between Type III and Type IV in the distances from the MTJ to the nerve entry points of USN and LSN in the neutral, external, or internal shoulder positions (Table 2).

**TABLE 1**. General Morphometric Parameters of the Type III and Type IV Subscapularis Muscles. Values are expressed as mean ± SD. Comparison between the right and left sides was performed using a paired t-test. $p \leq 0.05$ was considered statistically significant. Abbreviations: SSIBAA, Subscapularis superior–inferior belly axis angle; SD, standard deviation; mm, millimetres.

| Subscapularis muscle type | Parameter | Right side (Mean ± SD) | Left side (Mean ± SD) | P value |
|---|---|---|---|---|
| **Type III** | Footprint length | 26.07 ± 1.09 mm | 25.86 ± 1.05 mm | 0.472 |
| **Type IV** | Footprint length | 26.86 ± 0.88 mm | 26.62 ± 0.85 mm | 0.214 |
| **Type III** | Myotendinous junction width | 29.73 ± 1.43 mm | 29.53 ± 1.45 mm | 0.375 |
| **Type IV** | Myotendinous junction width | 31.04 ± 2.02 mm | 30.76 ± 1.91 mm | 0.256 |
| **Type III** | Scapular height | 144.51 ± 3.32 mm | 144.25 ± 3.42 mm | 0.306 |
| **Type IV** | Scapular height | 146.71 ± 2.58 mm | 146.47 ± 3.22 mm | 0.455 |
| **Type III** | Muscle height | 115.54 ± 2.65 mm | 115.27 ± 2.44 mm | 0.272 |
| **Type IV** | Muscle height | 118.31 ± 3.35 mm | 117.71 ± 2.53 mm | 0.105 |
| **Type III** | Subscapularis superior–inferior belly axis angle (SSIBAA) | 35.7 ± 1.77° | 35.6 ± 1.90° | 0.343 |
| **Type IV** | Subscapularis superior–inferior belly axis angle (SSIBAA) | 37 ± 1.63° | 36.69 ± 1.55° | 0.219 |

**TABLE 2:** Comparison of morphometric and neuroanatomical parameters between Type III and Type IV subscapularis muscles. Values are expressed as mean ± SD. Data from the right and left sides were pooled because no statistically significant bilateral differences were observed. Comparisons between Type III and Type IV muscles were performed using Welch's t-test. A P value ≤ 0.05 was considered statistically significant. Neuroanatomical measurements represent the linear shortest distances from the MTJ to the entry points of the USN and LSN, measured with the arm abducted to 30° in NR, ER, and IR. Abbreviations: SD, standard deviation; MTJ, myotendinous junction; USN, upper subscapular nerve; LSN, lower subscapular nerve; NR, neutral rotation; ER, external rotation; IR, internal rotation; mm, millimeters**.**

| **Morphometric parameters** | **Type III (Mean ± SD)** | **Type IV (Mean ± SD)** | ***P* values** |
|---|---|---|---|
| Footprint length | 25.96 ± 1.04 mm | 26.74 ± 0.85 mm | 0.011 |
| Myotendinous junction width | 29.63 ± 1.41 mm | 30.90 ± 1.93 mm | 0.013 |
| Muscle height | 115.41 ± 2.48 mm | 118.01 ± 2.93 mm | 0.002 |
| Scapular height | 144.38 ± 3.28 mm | 146.59 ± 2.86 mm | 0.022 |
| Subscapularis superior–inferior belly axis angle (SSIBAA) | 35.65° ± 1.79° | 36.88° ± 1.56° | 0.019 |
| Distance of the USN entry point from MTJ during NR | 27.89 ± 4.86 mm | 28.28 ± 5.35 mm | 0.796 |
| Distance of the USN entry point from MTJ during ER | 37.67 ± 5.08 mm | 37.91 ± 5.83 mm | 0.884 |
| Distance of the USN entry point from MTJ during IR | 20.79 ± 4.31 mm | 21.08 ± 4.65 mm | 0.827 |
| Distance of LSN entry point from MTJ during NR | 29.25 ± 5.06 mm | 29.93 ± 4.82 mm | 0.648 |
| Distance of LSN entry point from MTJ during ER | 36.74 ± 4.91 mm | 36.88 ± 5.06 mm | 0.923 |
| Distance of LSN entry point from MTJ during IR | 22.89 ± 4.48 mm | 24.17 ± 5.10 mm | 0.369 |

### 3.4 Tendon morphometry:

No significant difference was observed bilaterally in terms of tendon thickness, width, or length for either muscle type. In both Type III and Type IV SM, tendon thickness and width gradually decreased from the superior-most to the inferior-most tendon. In contrast, tendon length gradually increased in the same direction (Table 3). The results of the Bonferroni post hoc pairwise comparisons for tendon thickness, width, and length in both muscle types are presented in Table 4.

**TABLE 3:** Tendon morphometry of Type III and Type IV subscapularis muscles. Values are expressed as mean ± SD. Tendons were numbered sequentially from the superior-most (Tendon 1) to the inferior-most tendon. Morphometric parameters included tendon thickness, width, and length. Comparisons between the right and left sides were performed using a paired t-test. A P value ≤ 0.05 was considered statistically significant. Abbreviations: SD, standard deviation; mm, millimetres.

| Subscapularis muscle type | Tendon parameters | Right side (Mean ± SD) | Left side (Mean ± SD) | P value |
|---|---|---|---|---|
| **Type III** | Tendon 1 thickness | 3.43 ± 0.24 mm | 3.36 ± 0.24 mm | 0.073 |
| | Tendon 2 thickness | 3.21 ± 0.20 mm | 3.13 ± 0.23 mm | 0.089 |
| | Tendon 3 thickness | 3.04 ± 0.18 mm | 2.95 ± 0.16 mm | 0.096 |
| **Type IV** | Tendon 1 thickness | 3.41± 0.22 mm | 3.31 ± 0.21 mm | 0.076 |
| | Tendon 2 thickness | 3.13 ± 0.23 mm | 3.03 ± 0.22 mm | 0.091 |
| | Tendon 3 thickness | 3.0 ± 0.21 mm | 2.89 ± 0.19 mm | 0.115 |
| | Tendon 4 thickness | 2.88 ± 0.19 mm | 2.80 ± 0.16 mm | 0.193 |
| **Type III** | Tendon 1 width | 10.80 ± 0.84 mm | 10.72 ± 0.91 mm | 0.679 |
| | Tendon 2 width | 10.08 ± 0.68 mm | 10. 03 ± 0.66 mm | 0.770 |
| | Tendon 3 width | 8.89 ± 0.64 mm | 8.86 ± 0.81 mm | 0.890 |
| **Type IV** | Tendon 1 width | 10.23 ± 0.92 mm | 10.11 ± 0.86 mm | 0.368 |
| | Tendon 2 width | 8.63 ± 0.71 mm | 8.54 ± 0.82 mm | 0.624 |
| | Tendon 3 width | 6.72 ± 0.76 mm | 6.63 ± 0.62 mm | 0.750 |
| | Tendon 4 width | 5.60 ± 0. 59 mm | 5.56 ± 0.57 mm | 0.823 |
| **Type III** | Tendon 1 length | 40.17 ± 0.93 mm | 40.13 ± 0.93 mm | 0.802 |
| | Tendon 2 length | 41.75 ± 0.85 mm | 41.63 ± 0.85 mm | 0.584 |
| | Tendon 3 length | 41.88 ± 0.95 mm | 41.71 ± 0.95 mm | 0.519 |
| **Type IV** | Tendon 1 length | 40.18 ± 0.89 mm | 40.16 ± 0.80 mm | 0.792 |
| | Tendon 2 length | 41.65 ± 0.77 mm | 41.60 ± 0.82 mm | 0.695 |
| | Tendon 3 length | 41.86 ± 0.72 mm | 41.79 ± 0.75 mm | 0.675 |
| | Tendon 4 length | 41.99 ± 0.84 mm | 41.92 ± 0.82 mm | 0.542 |

**TABLE 4**. Bonferroni post hoc pairwise comparisons of tendon length, width, and thickness among tendons in Type III and Type IV subscapularis muscles. P values were obtained from Bonferroni-adjusted post hoc pairwise comparisons following one-way repeated-measures ANOVA. Analyses were performed separately for the right and left sides. A Bonferroni-adjusted P value < 0.0167 was considered statistically significant for Type III subscapularis muscles, whereas P < 0.0083 was considered statistically significant for Type IV subscapularis muscles. Abbreviations: Tendon 1–3, first to third tendons of Type III subscapularis muscles; Tendon 1–4, first to fourth tendons of Type IV subscapularis muscles.

| Parameter | Muscle type | Comparison | P value (right side) | P value (left side) |
|---|---|---|---|---|
| Tendon thickness | Type III | Tendon 1 vs Tendon 2 | 0.042 | 0.043 |
| | | Tendon 1 vs Tendon 3 | 0.0007 | 0.0003 |
| | | Tendon 2 vs Tendon 3 | 0.059 | 0.062 |
| | Type IV | Tendon 1 vs Tendon 2 | 0.005 | 0.002 |
| | | Tendon 1 vs Tendon 3 | < 0.0001 | < 0.0001 |
| | | Tendon 1 vs Tendon 4 | < 0.0001 | < 0.0001 |
| | | Tendon 2 vs Tendon 3 | 0.136 | 0.093 |
| | | Tendon 2 vs Tendon 4 | 0.005 | 0.005 |
| | | Tendon 3 vs Tendon 4 | 0.140 | 0.218 |
| Tendon width | Type III | Tendon 1 vs Tendon 2 | 0.049 | 0.067 |
| | | Tendon 1 vs Tendon 3 | 0.00002 | 0.00004 |
| | | Tendon 2 vs Tendon 3 | 0.0007 | 0.0006 |
| | Type IV | Tendon 1 vs Tendon 2 | < 0.0001 | < 0.0001 |
| | | Tendon 1 vs Tendon 3 | < 0.0001 | < 0.0001 |
| | | Tendon 1 vs Tendon 4 | < 0.0001 | < 0.0001 |
| | | Tendon 2 vs Tendon 3 | < 0.0001 | < 0.0001 |
| | | Tendon 2 vs Tendon 4 | < 0.0001 | < 0.0001 |
| | | Tendon 3 vs Tendon 4 | 0.0003 | 0.0003 |
| Tendon length | Type III | Tendon 1 vs Tendon 2 | 0.001 | 0.002 |
| | | Tendon 1 vs Tendon 3 | 0.001 | 0.002 |
| | | Tendon 2 vs Tendon 3 | 0.778 | 0.852 |
| | Type IV | Tendon 1 vs Tendon 2 | 0.0001 | 0.0001 |
| | | Tendon 1 vs Tendon 3 | 0.00002 | 0.00002 |
| | | Tendon 1 vs Tendon 4 | 0.00002 | 0.00002 |
| | | Tendon 2 vs Tendon 3 | 0.542 | 0.612 |
| | | Tendon 2 vs Tendon 4 | 0.329 | 0.388 |
| | | Tendon 3 vs Tendon 4 | 0.667 | 0.681 |

### 3.5 Muscle belly morphometry:

We did not notice any notable bilateral differences in muscle belly measurements for either muscle type. In both Type III and Type IV SM, muscle belly height gradually decreased from the superior-most to the inferior-most belly. In contrast, muscle belly length gradually increased from the superior-most to the inferior-most (Table 5). The results of the Bonferroni post hoc pairwise comparisons of muscle belly height and muscle belly length among the muscle bellies of both muscle types are presented in Table 6.

**TABLE 5:** Muscle belly morphometry of Type III and Type IV subscapularis muscles. Values are expressed as mean ± SD. Muscle bellies were numbered sequentially from the superior-most (Muscle belly 1) to the inferior-most. Morphometric parameters included muscle belly length and height. Comparisons between the right and left sides were performed using a paired t-test. A P value ≤ 0.05 was considered statistically significant. Abbreviations: SD, standard deviation; mm, millimetres.

| Subscapularis muscle type | Muscle belly parameter | Right side (Mean ± SD) | Left side (Mean ± SD) | P value |
|---|---|---|---|---|
| **Type III** | Muscle belly 1 length | 94.77 ± 3.29 mm | 94.63 ± 2.95 mm | 0.494 |
| | Muscle belly 2 length | 107.96 ± 3.10 mm | 107.90 ± 2.87 mm | 0.781 |
| | Muscle belly 3 length | 108.01 ± 2.99 mm | 107.86 ± 3.03 mm | 0.516 |
| **Type IV** | Muscle belly 1 length | 94.81 ± 2.50 mm | 94.61± 2.38 mm | 0.387 |
| | Muscle belly 2 length | 105.82 ± 2.41 mm | 105.74 ± 2.19 mm | 0.585 |
| | Muscle belly 3 length | 107.90 ± 2.33 mm | 107.82 ± 2.47 mm | 0.536 |
| | Muscle belly 4 length | 108.04 ± 2.53 mm | 107.90 ±2.38 mm | 0.410 |
| **Type III** | Muscle belly 1 height | 48.38 ± 3.08 mm | 48.23 ± 2.60 mm | 0.715 |
| | Muscle belly 2 height | 38.73 ± 2.68 mm | 38.66 ± 2.47 mm | 0.845 |
| | Muscle belly 3 height | 28.44 ± 2.07 mm | 28.38 ± 1.89 mm | 0.859 |
| **Type IV** | Muscle belly 1 height | 47.83 ± 2.74 mm | 47.60 ± 2.90 mm | 0.491 |
| | Muscle belly 2 height | 27.82 ± 2.25 mm | 27.60 ± 2.13 mm | 0.548 |
| | Muscle belly 3 height | 23.40 ± 2.16 mm | 23.17 ± 2.01 mm | 0.608 |
| | Muscle belly 4 height | 19.34 ± 1.46 mm | 19.25 ± 1.30 mm | 0.846 |

**TABLE 6**. Bonferroni post hoc pairwise comparisons of muscle belly length and height among muscle bellies in Type III and Type IV subscapularis muscles. P values were obtained from Bonferroni-adjusted post hoc pairwise comparisons following one-way repeated-measures ANOVA. Analyses were performed separately for the right and left sides. A Bonferroni-adjusted P value < 0.0167 was considered statistically significant for Type III subscapularis muscles and < 0.0083 for Type IV subscapularis muscles. Abbreviations: Belly 1–3, first to third muscle bellies in Type III subscapularis muscles; Belly 1–4, first to fourth muscle bellies in Type IV subscapularis muscles.

| Parameter | Muscle type | Comparison | P value (right side) | P value (left side) |
|---|---|---|---|---|
| **Muscle belly length** | Type III | Belly 1 vs Belly 2 | < 0.0001 | < 0.0001 |
| | | Belly 1 vs Belly 3 | < 0.0001 | < 0.0001 |
| | | Belly 2 vs Belly 3 | 0.972 | 0.974 |
| | Type IV | Belly 1 vs Belly 2 | < 0.0001 | < 0.0001 |
| | | Belly 1 vs Belly 3 | < 0.0001 | < 0.0001 |
| | | Belly 1 vs Belly 4 | < 0.0001 | < 0.0001 |
| | | Belly 2 vs Belly 3 | 0.035 | 0.032 |
| | | Belly 2 vs Belly 4 | 0.031 | 0.026 |
| | | Belly 3 vs Belly 4 | 0.888 | 0.952 |
| **Muscle belly height** | Type III | Belly 1 vs Belly 2 | < 0.0001 | < 0.0001 |
| | | Belly 1 vs Belly 3 | < 0.0001 | < 0.0001 |
| | | Belly 2 vs Belly 3 | < 0.0001 | < 0.0001 |
| | Type IV | Belly 1 vs Belly 2 | < 0.0001 | < 0.0001 |
| | | Belly 1 vs Belly 3 | < 0.0001 | < 0.0001 |
| | | Belly 1 vs Belly 4 | < 0.0001 | < 0.0001 |
| | | Belly 2 vs Belly 3 | < 0.0001 | < 0.0001 |
| | | Belly 2 vs Belly 4 | < 0.0001 | < 0.0001 |
| | | Belly 3 vs Belly 4 | < 0.0001 | < 0.0001 |

### 3.6 Origin and anatomical variations of the subscapular nerves:

The USN originated exclusively from the posterior cord (PC) in all specimens, demonstrating a highly consistent pattern of origin irrespective of SM type. However, variations in its branching pattern were common, with accessory upper subscapular nerves (aUSN) occurring more frequently in Type IV muscles and ranging from one to three additional branches. In contrast, the LSN exhibited considerable variability in its origin, arising from the PC, axillary nerve, or thoracodorsal nerve, whereas duplication of the LSN was observed only occasionally. Overall, the USN showed a constant origin but variable branching, whereas the LSN exhibited greater variability in its origin (Figure 4, Table 7).

**FIGURE 4**: **(a, b)** Cadaveric photographs showing the nerve innervation pattern of Type III and Type IV subscapularis muscles respectively. Numbers 1–4 indicate the corresponding muscle bellies in each muscle type. Abbreviations: BP, brachial plexus; PC, posterior cord; SSN, suprascapular nerve; USN, upper subscapular nerve; aUSN1, first accessory upper subscapular nerve; aUSN2, second accessory upper subscapular nerve; LSN, lower subscapular nerve; AN, axillary nerve; RN, radial nerve; TDN, thoracodorsal nerve.

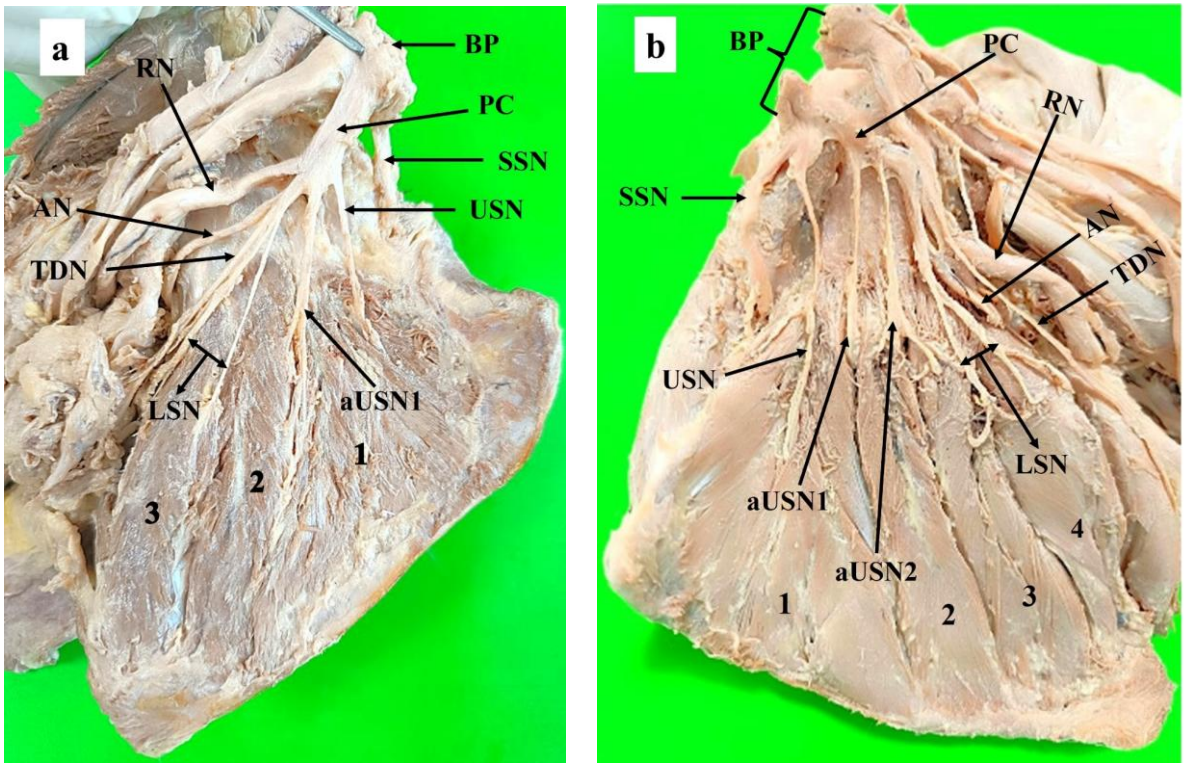


**TABLE 7**. Origin and anatomical variations of the upper and lower subscapular nerves in Type III and Type IV subscapularis muscles. Data are presented as the number of specimens. The origin of the USN and LSN was recorded as arising from the posterior cord, axillary nerve, or thoracodorsal nerve. Anatomical variations included accessory upper subscapular nerves and double lower subscapular nerves. A total of 20 Type III and 26 Type IV subscapularis muscles were examined. Right- and left-sided occurrences are indicated where applicable. Specimens with double LSN are also included in the corresponding nerve-origin category based on their site of origin.

† In two Type IV specimens with double LSN, both nerve branches originated from the axillary nerve.

‡ One Type III specimen with a double LSN had both branches originating from the thoracodorsal nerve.

Abbreviations: USN, upper subscapular nerve; LSN, lower subscapular nerve; R, right; L, left; n, number of specimens.

| **Nerve** | **Anatomical parameter** | **Type III (n = 20)** | **Type IV (n = 26)** |
|---|---|---|---|
| Upper subscapular nerve | Posterior cord origin | 20 | 26 |
| | Axillary nerve origin | 0 | 0 |
| | Thoracodorsal nerve origin | 0 | 0 |
| | One accessory USN | 6 (3R+3L) | 13 (7R+6L) |
| | Two accessory USNs | 1(R) | 4 (2R+2L) |
| | Three accessory USNs | 0 | 1 (R) |
| Lower subscapular nerve | Posterior cord origin | 10 | 12 |
| | Axillary nerve origin | 7 | 10† |
| | Thoracodorsal nerve origin | 3‡ | 4 |
| | Double LSN | 1 (R)‡ | 2 (1R+1L)† |

### 3.7 Association between muscle type and accessory upper subscapular nerves:

A significant association was observed between SM type and the presence of aUSN. The aUSN were significantly more frequent in Type IV muscles than in Type III muscles (69.2% vs. 35.0%; Pearson's $\chi^2$ (1) = 5.339, P = 0.021), demonstrating a significant association between Type IV SM morphology and the presence of aUSN (Figure 4, Table 8).

**TABLE 8**. Association between subscapularis muscle type and the presence of accessory upper subscapular nerves. Data are presented as counts and percentages of specimens. The association between subscapularis muscle type and the presence of accessory upper subscapular nerves was assessed using Pearson's chi-square test. A *P* value ≤ 0.05 was considered statistically significant. Abbreviations: USN, upper subscapular nerve; $\chi^2$, chi-square statistic; df, degrees of freedom; n, number of specimens.

| **Subscapularis muscle type** | **Accessory USN present, *n* (%)** | **Accessory USN absent, *n* (%)** | **Total (*n*)** |
|---|---|---|---|
| **Type III** | 7 (35.0) | 13 (65.0) | 20 |
| **Type IV** | 18 (69.2) | 8 (30.8) | 26 |
| **Total** | 25 (54.3) | 21 (45.7) | 46 |
| **Pearson $\chi^2$ (df = 1), P value** | 5.339, **0.021** | | |

### 3.8 Dynamic relationship between the myotendinous junction and the subscapular nerve entry points:

Measurements obtained with the shoulder abducted to 30° showed consistent positional changes in the USN and LSN during shoulder rotation. When accessory nerve branches of USN and LSN were present, analyses were based on the nearest nerve entry point to the MTJ. In both muscle types, the shortest straight-line distance from the MTJ to the nearest nerve entry point was greatest during external rotation, intermediate during neutral rotation, and shortest during internal rotation (Table 9). No significant bilateral difference was observed (Table 9). A one-way repeated-measures ANOVA with Bonferroni-adjusted post hoc analysis showed significant differences across all shoulder positions for both the USN and LSN (all P < 0.001) (Figure 5, Table 10). These findings showed that shoulder rotation significantly altered the distance between the MTJ and the nerve entry point.

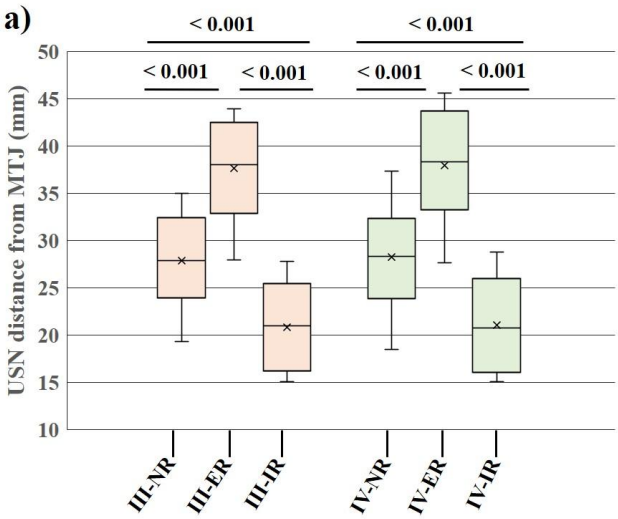
**TABLE 9:** Distance from the MTJ to the entry points of the upper and lower subscapular nerves in Type III and Type IV subscapularis muscles at different shoulder positions with the arm abducted to 30°. Values are expressed as mean ± SD. Measurements were obtained with the shoulder in NR, ER, and IR. Comparisons between the right and left sides were performed using a paired t-test. A P value < 0.05 was considered statistically significant. Abbreviations: MTJ, myotendinous junction; USN, upper subscapular nerve; LSN, lower subscapular nerve; NR, neutral rotation; ER, external rotation; IR, internal rotation; SD, standard deviation; mm, millimetres.

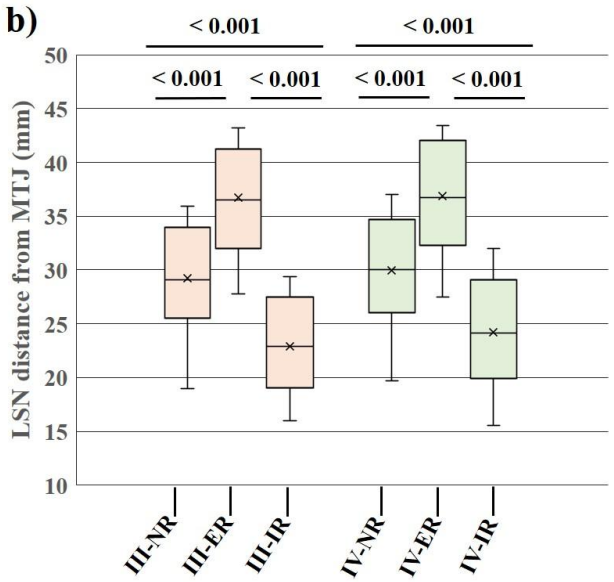
| Subscapularis muscle type | Nerve | Shoulder position | Right side (Mean ± SD) | Left side (Mean ± SD) | P value |
|---|---|---|---|---|---|
| Type III | USN | NR | 28.09 ± 4.99 mm | 27.69 ± 4.99 mm | 0.255 |
| | | ER | 37.72 ± 5.07 mm | 37.62 ± 5.36 mm | 0.704 |
| | | IR | 20.96 ± 4.46 mm | 20.63 ± 4.39 mm | 0.217 |
| Type IV | USN | NR | 28.42 ± 5.48 mm | 28.14 ± 5.43 mm | 0.424 |
| | | ER | 38.15 ± 6.03 mm | 37.67 ± 5.86 mm | 0.249 |
| | | IR | 21.14 ± 4.85 mm | 21.03 ± 4.63 mm | 0.849 |
| Type III | LSN | NR | 29.46 ± 4.98 mm | 29.04 ± 5.40 mm | 0.486 |
| | | ER | 36.74 ± 5.04 mm | 36.72 ± 5.05 mm | 0.963 |
| | | IR | 23.26 ± 4.56 mm | 22.52 ± 4.61 mm | 0.131 |
| Type IV | LSN | NR | 29.96 ± 4.95 mm | 29.89 ± 4.95 mm | 0.857 |
| | | ER | 36.93 ± 5.16 mm | 36.83 ± 5.10 mm | 0.808 |
| | | IR | 24.19 ± 5.37 mm | 24.16 ± 5.22 mm | 0.954 |

**TABLE 10:** Bonferroni post hoc pairwise comparisons of distances from the MTJ to the entry points of the upper and lower subscapular nerves across shoulder rotations (NR, ER, and IR) with the arm abducted to 30° in Type III and Type IV subscapularis muscles. P values were obtained using Bonferroni-adjusted post hoc pairwise comparisons following one-way repeated-measures ANOVA performed separately for Type III and Type IV subscapularis muscles. Data from the right and left sides were pooled because no significant bilateral differences were observed. A Bonferroni-adjusted P value < 0.0167 was considered statistically significant. Abbreviations: MTJ, myotendinous junction; USN, upper subscapular nerve; LSN, lower subscapular nerve; NR, neutral rotation; ER, external rotation; IR, internal rotation.

| **Subscapularis muscle type** | **Nerve** | **Pairwise comparison** | **P *value*** |
|---|---|---|---|
| **Type III** | USN | NR vs ER | < 0.0001 |
| | | NR vs IR | < 0.0001 |
| | | ER vs IR | < 0.0001 |
| **Type IV** | USN | NR vs ER | < 0.0001 |
| | | NR vs IR | < 0.0001 |
| | | ER vs IR | < 0.0001 |
| **Type III** | LSN | NR vs ER | 0.0001 |
| | | NR vs IR | 0.0001 |
| | | ER vs IR | < 0.0001 |
| **Type IV** | LSN | NR vs ER | 0.0001 |
| | | NR vs IR | 0.0001 |
| | | ER vs IR | < 0.0001 |

**FIGURE 5.** Box plots showing the distance from the MTJ to the entry points of (a) the USN and (b) the LSN, in Type III and Type IV subscapularis muscles, measured with the arm abducted to 30° in NR**,** ER**,** and IR**.** Boxes represent the interquartile range (IQR), the horizontal line within each box indicates the median, the cross (×) indicates the mean, and the whiskers represent the minimum and maximum values. Significant pairwise differences among shoulder positions within each muscle type were determined using one-way repeated-measures ANOVA followed by Bonferroni post hoc correction and are indicated above the box plots. Statistical significance was set at $P < 0.0167$ after Bonferroni correction. Abbreviations: MTJ, myotendinous junction; USN, upper subscapular nerve; LSN, lower subscapular nerve; NR, neutral rotation; ER, external rotation; IR, internal rotation; IQR, interquartile range; mm, millimetres.

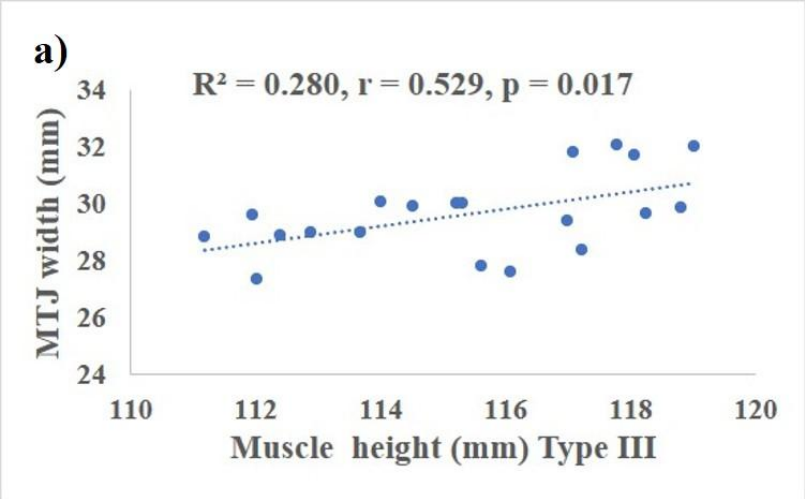


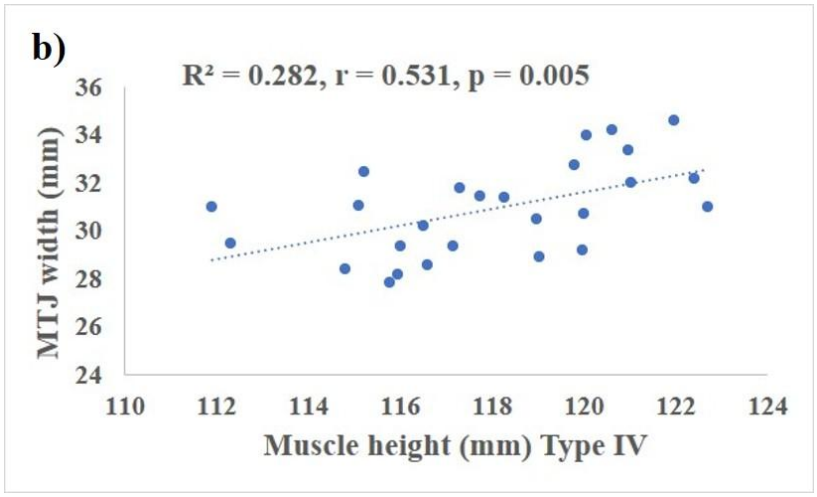



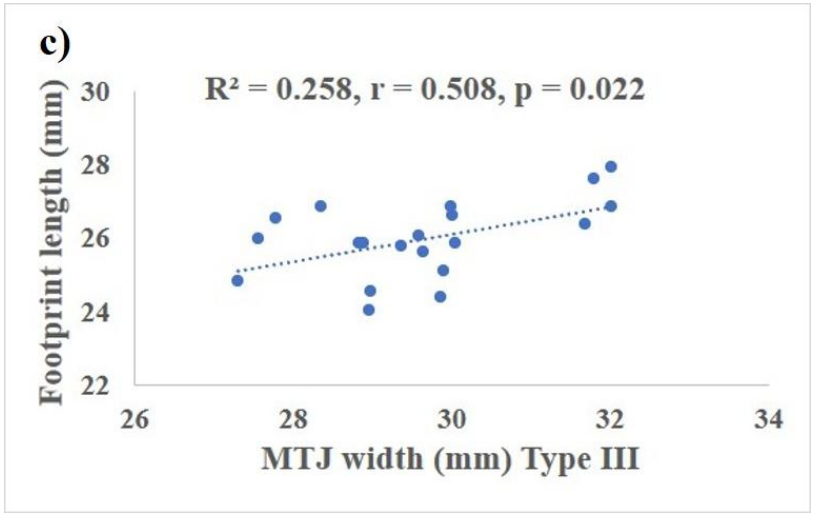
### 3.9 Correlation analysis:

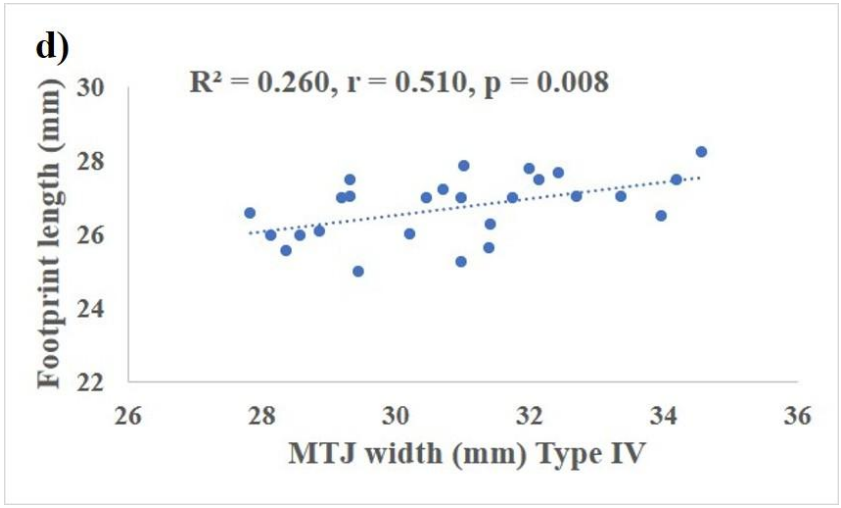
Pearson's correlation analysis demonstrated significant positive correlations between muscle height and MTJ width in both Type III ($R^2 = 0.280$, $r = 0.529$, $P = 0.017$) and Type IV SM ($R^2 = 0.282$, $r = 0.531$, $P = 0.005$). The MTJ width was positively correlated with footprint length in both Type III ($R^2 = 0.258$, $r = 0.508$, $P = 0.022$) and Type IV SM ($R^2 = 0.260$, $r = 0.510$, $P = 0.008$). In addition, a significant positive correlation was also observed between the scapular height and muscle height in both Type III ($R^2 = 0.389$, $r = 0.623$, $P = 0.003$) and Type IV SM ($R^2 = 0.391$, $r = 0.625$, $P = 0.0006$) (Figure 6, Table 11).

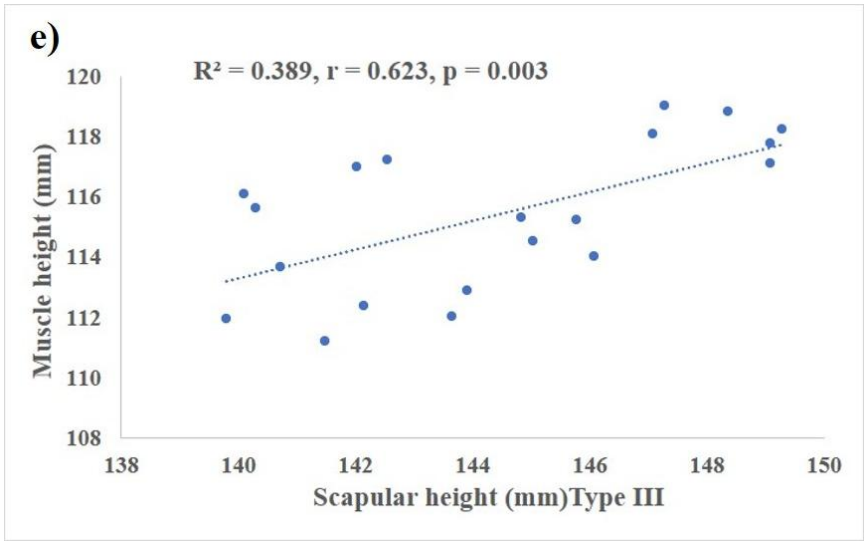
**FIGURE 6**: Scatter plots illustrating the relationships among selected morphometric parameters of Type III and Type IV subscapularis muscles. **(a)** Muscle height versus MTJ width in Type III muscles. **(b)** Muscle height versus MTJ width in Type IV muscles. **(c)** MTJ width versus footprint length in Type III. **(d)** MTJ width versus footprint length in Type IV. **(e)** Scapular height versus muscle height in Type III. **(f)** Scapular height versus muscle height in Type IV. The dotted lines represent the linear regression lines. Pearson's correlation coefficients (r), coefficients of determination ($R^2$), and corresponding P values are presented in each panel. Abbreviations: MTJ, myotendinous junction.




b)
R² = 0.282, r = 0.531, p = 0.005
MTJ width (mm)
36
34
32
30
28
26
24
110
112
114
116
118
120
122
124
Muscle height (mm) Type IV


c)
R² = 0.258, r = 0.508, p = 0.022
Footprint length (mm)
30
28
26
24
22
26
28
30
32
34
MTJ width (mm) Type III


d)
R² = 0.260, r = 0.510, p = 0.008
Footprint length (mm)
30
28
26
24
22
26
28
30
32
34
36
MTJ width (mm) Type IV


e)
R² = 0.389, r = 0.623, p = 0.003
Muscle height (mm)
120
118
116
114
112
110
108
138
140
142
144
146
148
150
Scapular height (mm)Type III

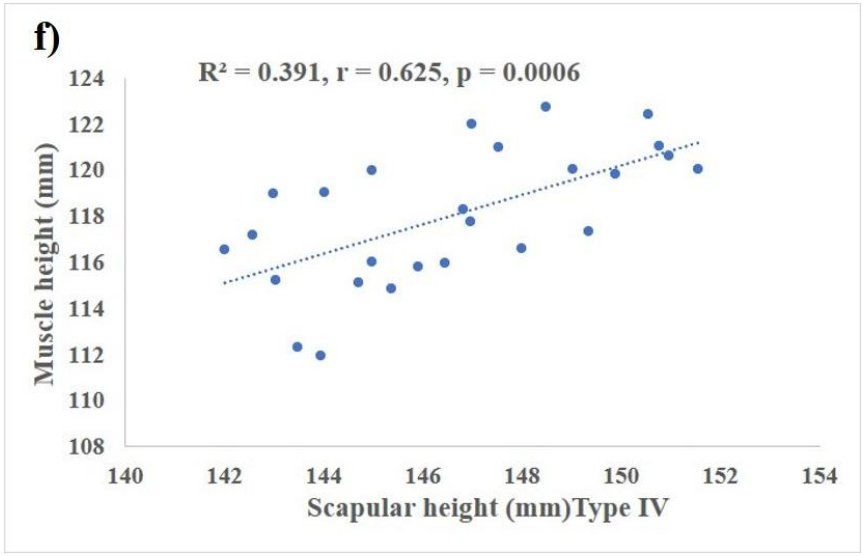

f)
R² = 0.391, r = 0.625, p = 0.0006
Muscle height (mm)
124
122
120
118
116
114
112
110
108
140
142
144
146
148
150
152
154
Scapular height (mm)Type IV

**TABLE 11**. Pearson's correlation analysis of selected morphometric parameters in Type III and Type IV subscapularis muscles. Values are presented as the Pearson correlation coefficient (r), coefficient of determination ($R^2$), and corresponding P value for each relationship. Positive r values indicate a positive linear correlation between the variables. Statistical significance was set at $P \leq 0.05$.

| Morphometric parameters | Type III ($R^2$) | Type III (r) | P | Type IV ($R^2$) | Type IV (r) | P |
|---|---|---|---|---|---|---|
| Muscle height vs. myotendinous junction width | 0.280 | 0.529 | 0.017 | 0.282 | 0.531 | 0.005 |
| Myotendinous junction width vs. footprint length | 0.258 | 0.508 | 0.022 | 0.260 | 0.510 | 0.008 |
| Scapular height vs. muscle height | 0.389 | 0.623 | 0.003 | 0.391 | 0.625 | 0.0006 |

**4 Discussion:** Our cadaveric study provides a comprehensive evaluation of the morphometry, innervation variability, and dynamic positional changes of the USN and LSN in Type III and Type IV SM. We found that,

- Type IV SM were more common than Type III in this series,
- Type IV SM had significantly greater footprint length, MTJ width, muscle height, scapular height, and SSIBAA than Type III SM,
- the USN consistently originated from the posterior cord, whereas the LSN showed considerable variability in its origin,
- aUSN were significantly associated with the Type IV SM,
- shoulder rotation produced consistent positional changes in the relationship between the MTJ and the subscapular nerve entry points; and
- Some morphometric parameters showed significant positive correlations, indicating proportional relationships among the measured parameters**.**

The SM is the biggest and most powerful component of the RC and shows considerable anatomical variability in its musculotendinous organization, origin and insertion points among the RC muscles (Pires et al. 2017). Previously, SM classification was based on either the number of muscle bellies or tendons. In both classifications, Type III and Type IV SM were found most commonly together. According to Zielińska et al. (2021), the three-bellied pattern (Type III) was marginally more prevalent than the four-bellied (Type IV) configuration (31.9% vs. 30.3%). In another study, considering the number of tendons, Zielińska et al. (2021) reported that Type IV was more frequently observed than Type III (39.1% vs. 7.8%). In their meta-analysis, Mann et al. (2022) also pointed out that these two types together account for most anatomical variations. They also reported an overall prevalence of Type IV of 57.4%, and of Type III of 27%. In this study, the prevalence of the Type IV pattern (56.5%) was higher than that of the Type III pattern (43.5%). Both muscle types showed normal anatomical variation. No specimens with developmental or pathological defects were identified.

A key finding of this study was that Type IV SM had a significantly larger musculotendinous architecture than Type III muscles. Greater footprint length, a wider MTJ, greater muscle height, a greater scapular height, and a greater SSIBAA collectively indicate a more extensive musculotendinous arrangement in Type IV SM (Tables 1 and 2). The reported footprint lengths ranged from 22.3 to 35.4 mm (Mann et al. 2023), 37.3 ± 4.6 mm (Gabardo et al. 2024), and 24.4 ± 5.7 mm (Sager et al. 2019). Zielińska et al. (2021) reported that the length of the scapular height averaged 143 mm and 148.48 mm in Type III and Type IV, respectively. They also observed muscle height of 110.74 mm and 118.7 mm for Type III and Type IV, respectively. In one study, the MTJ width was reported as 31.4 ± 2.6 mm in cadavers (Lafosse et al. 2018). Based on available English-language research, no studies have documented SSIBAA, so we could not directly compare our findings. The positive correlations observed among these parameters (Figure 6, Table 11) suggest that greater scapular height is associated with increased muscle height, which, in turn, is associated with a larger SSIBAA, a wider myotendinous junction, and a greater tendon footprint. Together, these findings indicate that these morphometric parameters are closely interrelated in the subscapularis muscle. A greater SSIBAA may accommodate more muscle fibers. This may increase the SM's physiological cross-sectional area (Charles et al. 2022). An increase in muscle cross-sectional area might increase its force-generating capacity. A larger humeral footprint provides a broader area for tendon insertion. This may allow multiple tendons to transmit force efficiently to their respective muscle bellies, facilitating complex, coordinated movements smoothly and providing dynamic stability of the GHJ. All this information may improve the anatomical and biomechanical understanding of the subscapularis musculotendinous complex.

In our study, we observed that the SM had multiple tendons and corresponding muscle bellies (Type III & Type IV). Analysis of tendon and muscle belly morphology revealed a highly organized architectural pattern in both muscle types. Tendon thickness and width progressively decreased from the superior-most to the inferior-most tendon, and muscle belly height also

decreased in a superior-to-inferior sequence. In contrast, tendon length and muscle belly length gradually increased from superior to inferior (Tables 3-6). Halder et al. (2000) mentioned that the thickness of the SM tendon decreased gradually from the superior (4.38 ± 1.01 mm) to the inferior (2.48 ± 0.79 mm) section of the tendon. The SM tendon thickness was recorded as 3.33 ± 1.14 mm (Arrillaga et al. 2024). Mann et al. (2023) reported that tendon thickness ranged from 2.4 to 9.1 mm and tendon length from 24.0 to 48.7 mm in cadavers. The SM had three tendons in 27% of cases and four tendons in 57.4% of cases (Mann et al. 2023). The length of the muscle belly was documented as 96.8–243.2 mm in cadavers (Mann et al. 2023). The average lengths of the first, second, and third muscle bellies of Type III were 87.19 mm, 98.51 mm, and 122.15 mm, respectively, whereas for the first, second, third, and fourth muscle bellies of Type IV they were 84.04 mm, 96.81 mm, 110.26 mm, and 120.92 mm, respectively (Zielinska et al., 2021). Similarly, the average muscle heights of the first, second, and third muscle bellies of Type III were 37.07 mm, 38.12 mm, and 35.55 mm, respectively, whereas for the first, second, third, and fourth muscle bellies of Type IV, the values were 28.99 mm, 29.75 mm, 29.11 mm, and 30.85 mm, respectively (Zielinska et al., 2021). The length of the muscle belly was gradually increased from superior to inferior (Zielinska et al. 2021), which also supports our findings. They reported maximum muscle belly lengths of 122.15 mm for Type III and 120.92 mm for Type IV SM. Lafosse et al. (2018) reported tendon and muscle belly lengths of 34.6 ± 5.6 mm and 138.6 ± 12.9 mm, respectively. In our study, we documented that the superior-most first tendon and muscle belly was the shortest of the others. The uppermost first tendon was also the thickest and widest among the lower tendons in both Type III and Type IV SM. The uppermost first belly also had the greatest muscle belly height compared with the lower muscle bellies in both Type III and Type IV (Tables 3, 5). During shoulder elevation, the uppermost muscle belly is most active compared with the lower muscle belly (Halder et al. 2000; Morag et al. 2011; Alilet et al. 2016; O'Connell et al. 2006). It plays a leading, powerful role in stabilizing the GHJ across various degrees of GHJ abduction. Meanwhile, the uppermost belly acts against the comparatively greater antigravity pull. This explains the complex action of this muscle, in which the uppermost belly performs an antigravitational action (abduction) while the lower bellies stabilize the GHJ in synergy with other RC muscles. The architecture of the uppermost belly thus accommodates a greater number of fibers of shorter length arranged in a pennate pattern, which is well adapted to the generation of greater force. This arrangement results in a manifold increase in physiological cross-sectional area (Charles et al.2022).

In this study, we observed that all USN originated from the posterior cord, whereas the emergence site of the LSN nerve was variable. The LSN arose from the posterior cord (PC), axillary nerve, or thoracodorsal nerve (Table 7). We also noted that the superior two-thirds of the SM was supplied by the USN and its accessory branches. In contrast, the LSN and its accessory branches innervated approximately the lower one-third of both Type III and Type IV SM muscle. Some prior studies have also documented the variable emergence patterns of the USN and LSN (Siwetz et al. 2020; Sager et al. 2019; Leschinger et al. 2016; Kasper et al. 2008; Tubbs et al. 2007). Tubbs et al. (2007) reported that USN arose from the PC of the brachial plexus in 97% of cases and from the axillary nerve in 3%. In contrast, the LSN arose from the PC in 79% of cases, and 21% of cases originated from the axillary nerve. They also observed

one aUSN in 8% of cases and two aUSN in 1.6% of cases, whereas one accessory lower subscapular nerve (aLSN) was present in 6.4% of cases in cadavers. Sager et al. (2019) documented that USN originated 100% from the posterior cord, but LSN arose from the posterior cord in 85% of cases and from the axillary nerve in 15% of cadavers. Leschinger et al. (2017) mentioned that subscapular nerves originated from the posterior cord, axillary nerve, and thoracodorsal nerve in 70%, 20%, and 10% of cadaveric specimens. They also observed that one accessory nerve for USN and LSN was found in 10% and 20% of cases, respectively. Kasper et al. (2008) documented that USN arose from the posterior cord in 70% of cases, and 30% were not specified. In contrast, the LSN originated from the posterior cord, axillary nerve, and thoracodorsal nerve in 65%, 25%, and 10% of cases, respectively. They also noted that 20% of cases had one aUSN and 15% had one aLSN. Saleh et al. (2012) mentioned that USN arose from the posterior cord in 100% of cases, whereas LSN originated from the posterior cord, axillary nerve, and thoracodorsal nerve in 81.8%, 15.2%, and 3%, respectively. Salah et al. (2012) documented that the frequency of occurrence of the accessory branches of the subscapular nerves varies from 48.5% for a single aUSN, 6.1% for double aUSN, 27.3% for a single aLSN, and 3% for a double aLSN. Siwetz et al. (2020) observed in their study that one aUSN was present in 9.7% of cases, and all arose from the posterior cord of the brachial plexus. A novel finding in this study was a significant association ($P = 0.021$) between aUSN and the Type IV muscle configuration compared with Type III. The aUSN was nearly twice as frequent in Type IV muscles as in Type III muscles, suggesting the presence of increased muscle fibers necessitating more neuronal innervation.

In the study, we have analyzed the dynamic relationship between the MTJ and the subscapular nerve entry points during shoulder rotation. We found that the distances measured between the innervation points of the USN and LSN and the MTJ were greatest during external rotation, intermediate during neutral rotation, and shortest during internal rotation across both SM types (Tables 2, 9, 10). The bilateral differences were nonsignificant in both nerves (Table 9). In the current study, we observed that the shortest straight-line distance from the nerves' entry points to the MTJ for USN and its accessory branches for both Type III and Type IV was $27.89 \pm 4.86$ mm and $28.28 \pm 5.35$ mm, respectively, at 30° of shoulder abduction during neutral rotation; $37.67 \pm 5.08$ mm and $37.91 \pm 5.83$ mm, respectively, for external rotation; and $20.79 \pm 4.31$ mm and $21.08 \pm 4.65$ mm, respectively, during internal rotation. Similarly, for LSN and its accessory branches for both Type III and Type IV, the corresponding values were $29.25 \pm 5.06$ mm and $29.93 \pm 4.82$ mm, respectively, at 30° of shoulder abduction during neutral rotation; $36.74 \pm 4.91$ mm and $36.88 \pm 5.06$ mm, respectively, for external rotation; and $22.89 \pm 4.48$ mm and $24.17 \pm 5.10$ mm, respectively, during internal rotation (Table 2). These findings indicated the dynamic association between the innervation points of the nerves and the MTJ. Some prior studies also documented dynamic shifts in the USN and LSN entry points in the SM during shoulder movement (Siwetz et al. 2022; Sager et al. 2019; Leschinger et al. 2017; Kasper et al. 2008). Kasper et al. (2008) reported that the distance between the entry point of the LSN, which originated from the posterior cord, and the GHJ was 35.9 mm for neutral rotation and 18.5 mm during maximum external rotation with zero-degree shoulder abduction. However, when the LSN originated from the axillary nerve, the distance during neutral rotation

became 36.6 mm, and for external rotation, 15.8 mm. The entry point of the USN from the MTJ was 23.7 ± 6.1 mm, and 24.3 ± 6.6 mm for LSN during external rotation of GHJ (Leschinger et al. 2017). Sager et al. (2019) reported that the USN entry point from the MTJ was 53.0 ± 14.7 mm during adduction with external shoulder rotation, 38.5 ± 9.7 mm during adduction with neutral rotation, and 30.0 ± 9.2 mm during adduction with internal shoulder rotation. They also reported the distance for LSN was 44.5 ± 13.8 mm during adduction with external shoulder rotation, 31.9 ± 9.3 mm during adduction with neutral rotation, and 25.4 ± 8.8 mm during adduction with internal shoulder rotation. The reported distance from the MTJ to the nerve insertion point during shoulder positioning as 24 to 64 mm for USN and 23 to 59 mm for LSN at 60° abduction and external rotation; 24 to 49 mm for USN and 15 to 43 mm for LSN at 60° abduction and internal rotation; and 26 to 54 mm for USN and 20 to 47 mm for LSN at 60° abduction and neutral rotation of the GHJ (Siwetz et al. 2022). The distance may be decreased (Kasper et al. 2008) or increased during external rotation from a reference point (Siwetz et al. 2022; Sager et al. 2019; Leschinger et al. 2017). In the current study, we also documented an increase in distance during external rotation and a decrease during internal rotation from the nerve entry point to the MTJ (Tables 2, 9,10). The differences in distance measured between the nerve entry points and the MTJ might be due to variations in measurement techniques, reference landmarks, and GHJ positioning. In this study, the minimum distance from the MTJ to the USN entry point with the arm abducted and externally rotated was 27.92 mm for Type III and 27.63 mm for Type IV SM. With the arm abducted and internally rotated, the minimum distance from the MTJ to the USN entry point was 15.06 mm for Type III and 15.07 mm for Type IV. Similarly, the minimum distance from the MTJ to the LSN entry point with the arm abducted and externally rotated was 27.8 mm for Type III and 27.5 mm for Type IV. With the arm abducted and internally rotated, the minimum distance from the MTJ to the LSN entry point was 16 mm for Type III and 15.58 mm for Type IV. Therefore, the anatomical safe zone with the arm abducted and externally rotated was approximately 27 mm medial to the MTJ for both SM types and both the USN and LSN, and approximately 15 mm with the arm abducted and internally rotated for both muscle types and both the USN and LSN. Siwetz et al. (2022) defined the anatomical safe zone for the USN and LSN with the arm abducted and externally rotated, extending up to 20 mm medial to the MTJ. Sager et al. (2019) defined the anatomical safe zone for USN with the arm adducted and externally rotated, extending up to 32 mm medial to the MTJ, and with the arm adducted and internally rotated, up to 18 mm. For LSN, the safe zone extended up to 26 mm from the MTJ with the arm adducted and externally rotated, and to 15 mm with the arm adducted and internally rotated.

a. **Clinical relevance:** We observed the dynamic USN and LSN entry point distance from the MTJ. Throughout the study, we maintained GHJ positioning at a standardized shoulder abduction angle of 30°. In the current study, we observed that during external rotation, the distance from the nerve entry point to the MTJ increased, and during internal rotation, it decreased compared with neutral GHJ rotation. Therefore, we hypothesized that external rotation of the GHJ may provide a greater safety margin than internal rotation for the USN and LSN. So, during the anterior GHJ approach, if the operating surgeons extend the dissection more medially and cross the anatomical safe

zone, it may injure the USN and LSN, which may lead to poor postoperative work performance by the SM. Hence, adequate and precise knowledge of the increased frequency of aUSN, the variable emergence pattern of LSN, and the dynamic relationship between the myotendinous junction and nerve entry points may guide surgeons in minimizing iatrogenic SM denervation during the anterior GHJ approach and other surgical procedures in the axillary region. In this study, we defined the anatomical safe zone during external rotation with arm abduction as up to 27 mm medial to the MTJ, and during internal rotation with arm abduction, it was 15 mm medial to the MTJ. All these observations furnish useful clinically relevant input regarding total GHJ arthroplasty, which is usually executed in a slightly abducted condition. Since the Type IV muscles have a larger musculotendinous architecture, they may also facilitate intraoperative identification of normal anatomical variants and improve preoperative interpretation of advanced imaging studies.

**b. Evolutionary perspective:**

Evolution likely influences the development of the subscapularis muscle's multipennate structure. The SM is like a monolithic structure with a single robust tendon in quadrupeds and their locomotion, for the purpose of weight bearing as a supportive function against the gravitational force. However, the SM evolves as a multi-tendinous structure in arboreal primates owing to more freedom of the upper limb (Zielińska et al. 2021). As modern humans became bipedal, the upper limbs became free, and more complex and precise GHJ movements led to the emergence of a multi-pennate SM with its tendons. The multi-pennate muscle belly with its individual tendon is an important evolutionary adaptation in humans, providing complex GHJ motion while ensuring dynamic stability. The multi-pennate arrangement of the SM may help prevent tendon tearing during complex GHJ movements owing to the distribution of the transmitted weight along its multiple tendons. Thus, the partial-thickness tendon tear is more common than the full-thickness tendon tear (Alilet et al. 2016). This would ensure that the person can perform normal GHJ activity without much difficulty. The partial tendon tear can be managed conservatively with painkiller medication, steroid injection, and physiotherapy. In non-traumatic cases, muscles with a single tendon are more prone to tear compared to those with multiple tendons (Mann et al. 2023). Less pennation and fewer tendons may provide greater stability of the shoulder joint, whereas more pennation with multiple tendons will provide less GHJ stability but facilitate complex and more precise movements of the GHJ.

**5 Strengths of the study:** The present study has several strengths. It furnished a detailed anatomical evaluation of the subscapularis muscle by combining morphometric measurements, tendon and muscle-belly architecture, SSIBAA, variations in the origin and branching of the subscapular nerves, dynamic association between the MTJ and the USN and LSN entry points during GHJ rotations, and correlation analysis between some morphometric parameters, all within a single cadaveric study. In the current study, we detailed various aspects of the SM that were not comprehensively reported in earlier published articles. Our study compares various

morphometric features of Type III and Type IV SM. The study also reported the variable innervation pattern of the subscapular nerves with greater association of the aUSN with Type IV SM. The dynamic association of the USN and LSN entry-point distance from the MTJ during shoulder rotations was also the highlight of this study. This information would impart valuable insights for surgeons performing anterior GHJ procedures. We followed meticulous dissection techniques, used well-defined anatomical landmarks, examined both sides, and kept measurements consistent to get accurate data. Overall, this study will provide detailed anatomical input that will be helpful in future research, imaging, and clinical use related to the subscapularis muscle. We also defined the anatomical safe zone to prevent injury to the subscapular nerves during the anterior GHJ surgical procedures.

## 6 Limitation:

This study has a few limitations. Because the research was conducted only on embalmed cadavers, the findings might not fully reflect living anatomy. As older adult cadavers were used, the findings could not reflect the younger population. Additionally, the dynamic measurements were performed under controlled cadaveric conditions and may not fully reflect the biomechanics of a living shoulder. We also did not study the correlations of body weight, sex, and height of the cadavers with the dynamic nerve entry points.

## 7 Conclusion:

In this cadaveric study, Type III and Type IV subscapularis muscles differed in musculotendinous architecture and showed distinct innervation patterns. Type IV muscles had significantly greater footprint length, myotendinous junction width, muscle height, scapular height, and SSIBAA than Type III muscles. The USN originated only from the posterior cord, whereas the LSN had variable origins. The aUSNs showed a much stronger association with Type IV muscles. Further, the position of the entry points of subscapular nerves relative to the myotendinous junction changed significantly with shoulder rotations, indicating that this relationship is dynamic. These findings improve our understanding of subscapularis morphology and its innervation. The findings of the study were not previously quantitatively demonstrated and may reflect an adaptive relationship between muscle architecture and its neural supply. Knowledge of the USN, LSN, and their accessory branches is crucial during surgical procedures around the GHJ. The small accessory branches can be easily overlooked during the anterior approach to the GHJ or during other operations in the axillary region. Even though the main nerve trunks are preserved, injury to these branches may compromise SM function. A sound understanding of the variable neuronal innervation pattern of the SM may help reduce the risk of iatrogenic nerve injury and improve post-operative surgical outcomes. We have attempted to define the anatomical safe zone for avoiding iatrogenic injury of the subscapular nerves as the orthopaedic surgeons make the anterior approach of GHJ, which should be limited up to 27 mm medial to the MTJ while keeping the arm externally rotated and abducted at 30 degrees. On the other hand, that safe zone should be limited to 15 mm medial to the MTJ during internal rotation of the arm in a similar abducted position. This understanding

would make a significant contribution to existing anatomical knowledge and its surgical implications.

**Declaration for the use of AI:** During the preparation of this manuscript, the authors used Grammarly to improve the text's clarity and grammar. The authors reviewed and edited the suggestions and take full responsibility for the final content.

**References:**


1. Alilet M, Behr J, Nueffer JP, Barbier-Brion B, Aubry S. Multi-modal imaging of the subscapularis muscle. Insights Imaging. 2016;7(6):779-791. doi: 10.1007/s13244-016-0526-1.
2. Arrillaga B, Miguel-Pérez M, Möller I, Rubio L, Blasi J, Pérez-Bellmunt A, Ortiz-Sagristà JC, Ortiz-Miguel S, Martinoli C. Human shoulder anatomy: new ultrasound, anatomical, and microscopic perspectives. Anat Sci Int. 2024;99(3):290-304. doi: 10.1007/s12565-024-00775-5.
3. Charles J, Kissane R, Hoehfurtner T, Bates KT. From fibre to function: are we accurately representing muscle architecture and performance? Biol Rev Camb Philos Soc. 2022;97(4):1640-1676. doi: 10.1111/brv.12856.
4. Gabardo S, Valencia-Mora M, Coifman I, Calvo E. Surgical anatomical landmarks for arthroscopic repair of subscapularis tendon tears. Clin Shoulder Elb. 2024;27(3):272-277. doi: 10.5397/cise.2023.01165.
5. Halder A, Zobitz ME, Schultz E, An KN. Structural properties of the subscapularis tendon. J Orthop Res. 2000;18(5):829-34. doi: 10.1002/jor.1100180522.
6. Kasper JC, Itamura JM, Tibone JE, Levin SL, Stevanovic MV. Human cadaveric study of subscapularis muscle innervation and guidelines to prevent denervation. J Shoulder Elbow Surg. 2008;17(4):659-62. doi: 10.1016/j.jse.2007.11.013.
7. Kasper JC, Itamura JM, Tibone JE, Levin SL, Stevanovic MV. Human cadaveric study of subscapularis muscle innervation and guidelines to prevent denervation. J Shoulder Elbow Surg. 2008;17(4):659-62. doi: 10.1016/j.jse.2007.11.013.
8. Lafosse T, Le Hanneur M, Lee J, Elhassan B. Bipolar pedicled teres major transfer for irreparable subscapularis tendon tears: an anatomic feasibility study. J Shoulder Elbow Surg. 2018;27(5):931-939. doi: 10.1016/j.jse.2017.11.024.
9. Leschinger T, Hackl M, Zeifang F, Scaal M, Müller LP, Wegmann K. Nerve supply of the subscapularis during anterior shoulder surgery: definition of a potential risk area. Arch Orthop Trauma Surg. 2017;137(1):135-140. doi: 10.1007/s00402-016-2585-7.
10. Mann MR, Plutecki D, Janda P, Pękala J, Malinowski K, Walocha J, Ghosh SK, Balawender K, Pękala P. The subscapularis muscle: A meta-analysis of its variations, prevalence, and anatomy. Clin Anat. 2023;36(3):527-541. doi: 10.1002/ca.24008.
11. Morag Y, Jamadar DA, Miller B, Dong Q, Jacobson JA. The subscapularis: anatomy, injury, and imaging. Skeletal Radiol. 2011;40(3):255-69. doi: 10.1007/s00256-009-0845-0.
12. O'Connell NE, Cowan J, Christopher T. An investigation into EMG activity in the upper and lower portions of the subscapularis muscle during normal shoulder motion. Physiother Res Int. 2006;11(3):148-51. doi: 10.1002/pri.336.

13. Pires LAS, Souza CFC, Teixeira AR, Leite TFO, Babinski MA, Chagas CAA. Accessory subscapularis muscle - A forgotten variation? Morphologie. 2017;101(333):101-104. doi: 10.1016/j.morpho.2017.04.003.
14. Preuss FR, Fossum BW, Peebles AM, Eble SK, Provencher MT. Subscapularis repair in reverse total shoulder arthroplasty: a systematic review and descriptive synthesis of cadaveric biomechanical strength outcomes. JSES Rev Rep Tech. 2022;2(4):437-441. doi: 10.1016/j.xrrt.2022.05.006.
15. Sager B, Gates S, Collett G, Chhabra A, Khazzam M. Innervation of the subscapularis: an anatomic study. JSES Open Access. 2019;3(2):65-69. doi: 10.1016/j.jses.2019.02.001.
16. Saleh DB, Callear J, McConnell P, Kay SP. The anatomy of the subscapular nerves: a new nomenclature. J Plast Reconstr Aesthet Surg. 2012;65(8):1072-5. doi: 10.1016/j.bjps.2012.03.020.
17. Siwetz M, Hammer N, Ondruschka B, Kieser DC. Variations in Subscapularis Muscle Innervation-A Report on Case Series. Medicina (Kaunas). 2020;56(10):532. doi: 10.3390/medicina56100532.
18. Siwetz M, Kieser D, Ondruschka B, Pretterklieber B, Hammer N. Is There a Nerve-free Zone in Which a Subscapularis Split Can Safely be Performed? An Anatomical Study Using Embalmed Specimens. Clin Orthop Relat Res. 2022;480(12):2432-2438. doi: 10.1097/CORR.0000000000002326.
19. Tubbs RS, Loukas M, Shahid K, Judge T, Pinyard J, Shoja MM, Slappey JB, McEvoy WC, Oakes WJ. Anatomy and quantitation of the subscapular nerves. Clin Anat. 2007;20(6):656-9. doi: 10.1002/ca.20478.
20. Virk MS, Aiyash SS, Frank RM, Mellano CS, Shewman EF, Wang VM, Romeo AA. Biomechanical comparison of subscapularis peel and lesser tuberosity osteotomy for double-row subscapularis repair technique in a cadaveric arthroplasty model. J Orthop Surg Res. 2019;14(1):391. doi: 10.1186/s13018-019-1372-x.
21. Walley KC, Saloky KL, Updegrove GF, Lopez H, Armstrong AD. Characterization of an anatomic safe zone surrounding the lower subscapular nerve during an open deltopectoral approach. J Shoulder Elbow Surg. 2019;28(4):671-677. doi: 10.1016/j.jse.2018.09.008.
22. Zielinska N, Olewnik Ł, Karauda P, Tubbs RS, Polguj M. A very rare case of an accessory subscapularis muscle and its potential clinical significance. Surg Radiol Anat. 2021;43(1):19-25. doi: 10.1007/s00276-020-02531-6.
23. Zielińska N, Tubbs RS, Borowski A, Podgórski M, Olewnik Ł. The Subscapularis Muscle: A Proposed Classification System. Biomed Res Int. 2021; 2021:7450000. doi: 10.1155/2021/7450000.
24. Zielińska N, Tubbs RS, Podgórski M, Karauda P, Polguj M, Olewnik Ł. The subscapularis tendon: A proposed classification system. Ann Anat. 2021; 233:151615. doi: 10.1016/j.aanat.2020.151615.